Development and analysis of friction material for eco-friendly brake pad using seashell composite

A. Adekunle[a], M. Okunlola[a], P. Omoniyi[a,b,*], A. Adeleke[c], P. Ikubanni[d], T. Popoola[a], and H. Ibrahim[a]

a. *Department of Mechanical Engineering, University of Ilorin, Ilorin 240003, Nigeria.*
b. *Department of Mechanical Engineering Science, University of Johannesburg, Johannesburg 2092, South Africa.*
c. *Department of Mechanical Engineering, Nile University of Nigeria, Abuja 90001, Nigeria.*
d. *Department of Mechanical Engineering, Landmark University, Omu-Aran 251101, Nigeria.*

Abstract. Asbestos remains banned in many countries as a result of its negative effects on the environment and human health. As a result, a human-friendly friction material is required to replace asbestos in brake pads. Hence, the powder metallurgy technique was undertaken to develop friction material from locally sourced asbestos-free materials. Seashell was used as base elements with other additives. The considered filler material had a particulate size of 300 μm, and epoxy resin was used as a binder. The produced brake pads were evaluated and compared to commercial brake pads in terms of their physical, mechanical, and tribological properties. According to the investigated properties of the developed brake pads, increasing the seashell content in the formulated brake pads resulted in a decrease in wear rate and compressive strength. Water absorption, hardness, oil absorption, density, and thermal conductivity all varied differently at the same time. The coefficient of friction of the produced friction material ranges between 0.311 and 0.353. The results showed that seashell particles could effectively replace asbestos in producing friction material for brake pads in an automobile.

1. Introduction

A brake acts as a mechanical device that prevents motion by absorbing the energy of a moving system

*. *Corresponding author. Tel.: +2348135910454*
E-mail addresses: adekunlebayo@yahoo.com (A. Adekunle);
mojeed_uthman91@yahoo.com (M. Okunlola);
omoniyi.po@unilorin.edu.ng (P. Omoniyi);
adeleke.kunle@ymail.com (A. Adeleke);
ikubanni.peter@lmu.edu.ng (P. Ikubanni);
tomtomleet@yahoo.co.uk (T. Popoola);
ibrahim.kh@unilorin.edu.ng (H. Ibrahim)

[1–3]. It is used to slow or stop a moving vehicle's wheel or to inhibit their motion, most commonly through friction [4]. For all vehicles equipped with brake discs, brake pads represent an essential and important component of the disc braking system [5]. The brake pad uses pressure from the pedal through fluid to the caliper containing the pads, forcing the friction material against the disc connected to the wheel. The wheel rotation is altered by absorbing the kinetic energy of the wheel. The kinetic energy in the form of heat is dissipated to the surrounding [1,2].

Brake pads consist of four major materials: Binders, fillers, friction materials, and reinforcements [3–6]. Friction materials play an important role in the

brake system since the pad's crucial part decelerates and stops the wheel's rotation and is mainly made of composite materials [7,8]. In the past, asbestos was used as the frictional material in brake pads. However, because asbestos is now banned in many countries due to its carcinogenic nature, its use is discouraged [9,10]. Furthermore, at 200°C, the efficacy of the asbestos brake pad is reduced [11]. Several researchers have replaced the carcinogenic asbestos-lined brake pads in the market with eco-friendly materials, such as palm kernel shells [12], periwinkle, sawdust, cow hooves, cow horn, bananas peels, and eggshell, together with other additives. However, one of the materials that has shown tremendous potential for friction material production is seashell. Seashell is the exoskeleton of an invertebrate composed of up to 96.8% calcium carbonate [13]. Seashells can be found at the reach of beaches in the United States, Australia, and the sub-region of Africa, excluding Nigeria.

A study has investigated the use of palm kernel fiber as a replacement for asbestos, and has found that a replacement rate of up to 5% is suitable due to its excellent tribological properties in brake pads [12]. In comparison, Bernard and Jayakumari [14] reported 8% palm fiber to give an optimum tribological property. a study has found that the use of areca sheath fiber is suitable for brake pads, with a 5% addition of areca sheath demonstrating good tribological properties compared to higher percentage additions [15]. Generally, the use of alternative frictional materials has shown improved tribological properties over asbestos brake pads. The use of Multiwall Carbon Nanotubes (MWCNT) and aluminum magnesium alloys with Nickel Sulfate ($NiSO_4$) as filler materials in the manufacturing of brake pads has been shown to improve their tribological and mechanical properties [4,16,17]. However, these materials come at a high price and are not readily available in the developing world.

As a result, the purpose of this article is to investigate the physicomechanical and tribological properties of brake pads made with seashells as frictional material and compare them to aftermarket products. The availability, cost of material, and properties are the primary considerations in choosing the materials for developing the brake pad.

2. Materials and method

The materials used in this study were seashell (friction material), palm kernel shell, and metal chips (reinforcement), sawdust, charcoal (filler), and epoxy resin and hardener (Diethylenediamine)(binders). The seashells were collected from Eleko beach, Ajah Lagos State, Nigeria. The sawdust from Tectona Grandis, commonly known as teak wood, was obtained from Tanke

sawmill located along the University of Ilorin Road in Ilorin. The palm kernel shell, on the other hand, was collected from Iyeku, which is situated in Odo-Otin South Local Government of Osun State. Metal chips of high carbon steel with a carbon content of 0.72% were collected from the Mechanical Engineering Department Central Laboratory, University of Ilorin and were sieved with apertures of 1.7 mm. Epoxy resin and hardener were purchased from the Ojota chemical market (Lagos), and charcoal was purchased at Gago junction, Tanke oke-odo, Ilorin.

The seashell, sawdust, palm kernel shell, and charcoal were sundried for three days (5 h/day) to remove excess moisture. They were pulverized using a hammer mill and were sieved into particle sizes of 300 μm, 300 μm, 300 − 150 μm, and 300 μm (Figure 1).

The samples in the proportion shown in Table 1 (seashell fines, sawdust fines, metal chips, palm kernel shell fines, and charcoal fines) were mixed thoroughly to achieve homogeneity using a mechanical mixer at the speed of 600 rpm for ten minutes. The epoxy resin and hardener (2:1) were homogeneously mixed in a separate container. The mixtures were then blended to obtain a low moisture composition mixture. The blended mixture was transferred into a fabricated metallic mold. A force of 40 kN was applied to compress the material with a holding time of ten minutes under a hydraulic compression machine. The compression machine was then released and the molded sample was ejected from the mold and left to dry at room temperature for 48 hours before transferring to an oven and cured for 60 minutes at 150°C. As shown in Figure 2, the cured samples were cooled at room temperature and placed in a zip-locked bag for preservation before further analysis.

2.1. Density
The Archimedes' principle is used to calculate the volume and density of an irregularly shaped object by measuring its mass in air and practical volume when submerged in water [5,18]. A small sample was cut off, weighed in air as W (g), and then submerged in a graduated cylinder filled with water. The volume of water displaced was recorded as V (cm^3). The density is expressed and shown in Eq. (1) [18]:

$$Density = \frac{W}{V}, \tag{1}$$

where W denotes the weight of sample in air and V is the volume of water displaced. The unit of density is g/cm^3.

2.2. Oil and water absorption
Oil and water absorption tests were carried out to determine sample vulnerability and porosity when submerged in water and oil for a specified period of time.

Figure 1. Photographs of ground materials: (a) Seashell fines, (b) sawdust fines, (c) palm kernel shell, (d) charcoal fines, (e) metal chips, and (f) epoxy resin and hardener.

Table 1. The proportion of materials for production of brake pad.

Sample	Seashell (g)	Sawdust (g)	Palm kernel shell (g)	Charcoal (g)	Metal chips (g)	Binder (g)	Total (%)
A	15	35	3	10	10	27	100
B	20	30	5	8	10	27	100
C	25	25	7	6	10	27	100
D	30	20	9	4	10	27	100
E	35	15	11	2	10	27	100

Figure 2. Samples of the produced brake pads.

In order to determine the absorption properties of the brake pad, Eq. (2) was used. The oil used was SAE40 automotive engine oil. For 168 hours, the samples were immersed in water and oil (7 days). Specimens were removed from the water and oil, thoroughly cleaned to remove any remaining water and oil from the surfaces, and reweighed to determine the new weights recorded as W_f. Eq. (2) was then used to calculate the percentage absorptions [9,19,20]:

$$Absorption(\%) = \frac{W_f - W_i}{W_i} \times 100, \qquad (2)$$

where W_i is the weight before immersion and W_f is the weight after immersion.

2.3. Hardness test

The hardness test was performed with the aid of Monsanto testing machine for hardness and shearing to determine the Brinell hardness of samples. The spherical indenter is 10.00 mm in diameter. Samples were cut into specific sizes and fixed into the tensiometer. A compression load of 1250 kg for 20 seconds was applied. The indented diameter was measured by eye scope [21]. Eq. (3) is used to calculate the Brinell hardness (BHN) [22].

$$BHN = \frac{W}{\left(\frac{\pi D}{2}\right) \times \left(D - \sqrt{D^2 - d^2}\right)}, \qquad (3)$$

where W denotes the load on the indenter (kg), D

Table 2. Properties of friction materials.

Sample/property	A	B	C	D	E	Control
Density (g/cm^3)	1.198	1.030	0.884	1.015	0.962	1.533
Water absorption (%)	41.7700	31.7680	28.2230	20.2470	14.5140	3.113
Oil absorption (%)	28.6170	20.3350	16.5940	13.326	06.8630	3.103
Hardness (BHN)	6.3	15.6	36.9	57.4	67.2	154.3
Specific wear rate (mm^3/Nm)	0.186	0.354	0.151	0.0614	0.0740	0.0812
COF	0.351	0.311	0.352	0.315	0.353	0.318
Thermal conductivity (W/m°C)	3.118	2.494	3.501	2.799	5.261	3.161
Compressive strength (MPa)	59.52491	51.73037	28.00349	17.74132	14.32324	13.837

the diameter of the steel ball (mm), and d the average measured diameter of the indentation (mm).

2.4. Abrasion resistance/wear rate test

An abrasion resistance test was carried out using the pin-on-disc weight loss/wear test machine. A load of 20 N was applied on the stylus pin for 200 cycles. After the cycle was completed, the sample was removed from the specimen holder and reweighed [9]. The specific wear rate was expressed in Eq. (4) and the test was carried out according to ASTM G99 [16,23]:

$$W_s = \frac{\Delta V}{F \times S},\qquad(4)$$

where W_s denotes the specific wear rate (mm^3/Nm), V volume loss (mm^3), F the applied load (N), and S the sliding distance (m).

2.5. Friction coefficient test

An inclined plane was used to perform the coefficient of friction test. The standard specifies that the frictional coefficient of each sample be determined using an inclined angle (α) tilted and fixed at 40°. A small hole was made on the brake pads, and a thread of negligible weight was attached to the weighted sample (F). The thread was then passed across a frictionless, grooved pulley and connected to the weight hanger. The weight hanger load steadily increased until the pad slid at a constant velocity. The load was recorded as (X) and the coefficient of friction was calculated. The coefficient of friction was computed using Eqs. (5) and (6) [24]:

$$W = m \times a = m \times g,\qquad(5)$$

where W is weight of sample; $a = g =$ acceleration due to gravity; and m is mass of pad.

$$\mu = \frac{X - F \sin\alpha}{F \cos\alpha},\qquad(6)$$

where μ is the coefficient of friction.

2.6. Thermal conductivity test

The Armfield computer compatible linear heat conduction accessory HT11C was used for this experiment. The specimens were prepared at average diameters of 30 mm and 5 mm to accommodate the equipment.

2.7. Compression strength test

A compression test was also performed on the samples using a universal testing machine (Model: INSTRON 3369) [25,26]. All tests were carried out following ASTM D3410 [27].

2.8. Scanning Electron Microscopy (SEM) and Energy-Dispersive X-Ray Fluorescence (ED-XRF) Spectrometry

The distribution of the materials in the brake pad was determined using SEM analysis. The elemental composition of the composite was determined using the ED-XRF.

3. Results and discussion

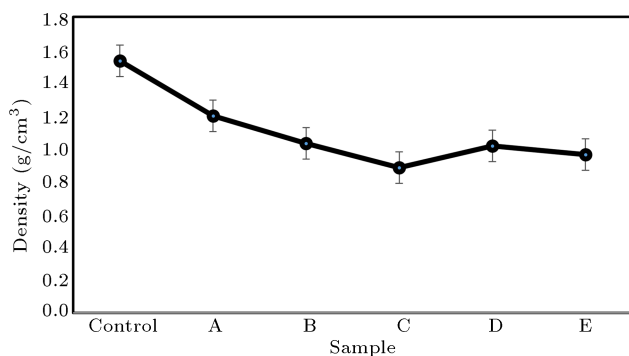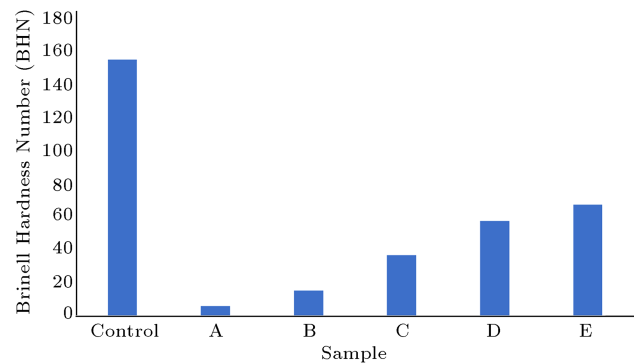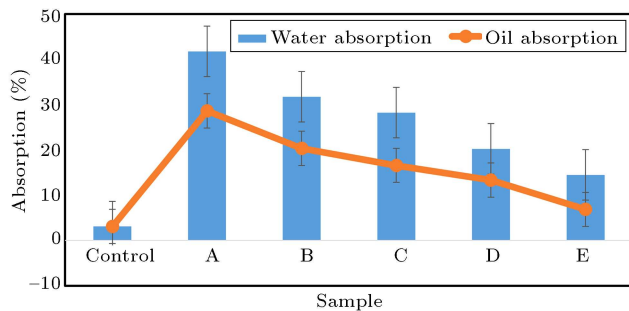### 3.1. Physico mechanical and Tribological properties

Table 2 compares the properties of the developed composite brake pad to those of the existing brake pad in the market. Table 3 presents a comparison of the physicomechanical and tribological properties between sample D and the brake pad material currently available in the market, which is referred to as the control sample.

3.1.1. Density assessment

Figure 3 depicts the density of the produced brake pads in comparison to the control sample. It was discovered that increasing the number of seashells in the formulated samples lead to the reduced density. The decrease in density could be attributed to the low density of seashells, which increased the composition of the materials. They are lighter in weight and meet the criteria of Standard Organization of Nigeria (SON)

Table 3. Summary of results of sample (D) compared with the control/commercial sample.

Property	Control sample	Produced sample
Density (g/cm^3)	1.533	1.015
Water absorption (%)	3.113	20.247
Oil absorption (%)	3.103	13.326
Hardness (BHN)	154.3	57.4
Specific wear rate (mm^3/Nm)	0.0812	0.0614
Coefficient of friction	0.318	0.315
Thermal conductivity (W/m°C)	3.161	2.799
Compressive strength (MPa)	13.837	17.741

Figure 3. Comparison of density of the produced samples with the control brake pad material.

Figure 5. Comparison of the hardness of the produced samples with the control brake pad.

Figure 4. Comparison of water/oil absorption of the produced samples with the control brake pad.

specifications. The brake pads developed in this study have a similar density to those reported by Popoola et al. [24] for brake pads produced using palm kernel shell, coconut shell, sea shell, and cow bone. Lower density suggests higher quality than conventional friction material used in brake pad applications, as reported by Edokpia et al. [22].

3.1.2. Absorption assessment
Figure 4 depicts the sample percentages of water and oil absorption. Water and oil absorption decreased from sample A to sample E, indicating that the higher the seashell content in the formulation, the less water and oil absorption. Sample E has the lowest water/oil

absorption of 14.51/6.86%, while the control sample has 3.11/3.10%. The higher value of water and oil absorption of the produced samples is attributed to the presence of voids in the samples and is reduced by increasing the compressing force. Furthermore, the reduction in oil and water absorption due to increased seashell content could be attributed to the impermeability nature of seashells. Also, the interfacial bonding energy provided by the binder contributed to the less porosity observed as the seashell content increased. This was also observed by Achebe et al. [6] who used palm kernel shell as filler material. Generally, all the produced samples exhibit improved water/oil absorption compared to that of the commercial sample.

3.1.3. Hardness assessment
Figure 5 depicts the hardness behavior of the produced brake pads and the control sample. It was discovered that as the seashell content in the formulation increased, the hardness of the material increased uniformly. The hardness value of each composite specimen is lower than that of the control friction material. The low hardness values obtained in all the produced samples could be attributed to the decreased bonding strength and the intermolecular bonding within the composite material. The hardness value of the control friction material is 154.3 BHN, while the highest

hardness value of the produced samples is 67.2 BHN, while the lowest hardness is 6.3 BHN. These results were in line with reports of Achebe et al. [6], where an increase in palm kernel particles as a replacement of asbestos increased hardness.

3.1.4. Wear (abrasion) resistance assessment
The specific wear rate of composite specimens and the control sample is depicted in Figure 6. The specific wear rate of specimens was reduced as the seashell content increased and could be attributed to the high hardness of seashells. Furthermore, the calcium carbonate present in the seashell acts as a binding material just like cement, thereby improving the wear rate of the composite [13]. Also, Park et al. [28] attributed resistance to the wear of seashells to the film formed by carbon carbonate. The specific wear rate decreased from sample B to D, with hardness values ranging from 15.6 to 57.4 BHN and specific wear rates ranging from 0.497 to 0.0831. The specific wear rate of the control sample is 0.0812 with a hardness value of 154.3 BHN. An increase in seashell content resulted in a reduction in the effectiveness of the binder to bind the composite under a compressive force of 40 kN. Sample D demonstrates the best friction material composition because it has the highest wear resistance of all the samples produced. The sliding distance is critical in determining the specific wear rate as a greater sliding distance results in a lower wear rate. The equivalent specific wear rate at the same sliding distance reveals that the specific wear rate of sample D at the same sliding distance has greater wear resistance than the control brake pad material. Sample D has a specific wear rate of 0.0614, which is 32.25% higher than the control sample, which has a specific wear rate of 0.0812. The results show that the specific wear rates of sample D outperform the control sample. Furthermore, the Archard wear model [17] stipulates that the volume of material removal is inversely proportional to the hardness of the material and was further corroborated
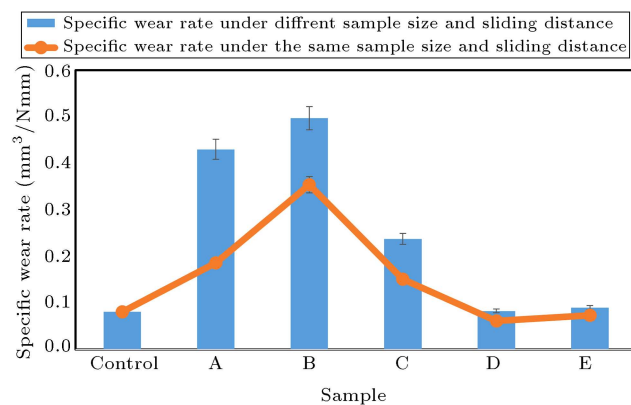
by Ezekiel and Inambao [29]. This phenomenon was observed in the brake pad material, where the higher hardness of the control sample resulted in a lower wear rate of the sample.

3.1.5. Coefficient of friction assessment
Figure 7 presents the coefficient of friction of produced brake pads and the control brake pad. It is shown that samples A, C, and E have the same coefficient of friction (μ) of 0.35, and samples B and D have $\mu = 0.311$ and 0.315, respectively. These results can be attributed to the distribution of seashells in the samples. From the results, it can be deduced that sample D ($\mu = 0.315$) has the closest coefficient of friction to the control sample ($\mu = 0.318$). The competitive friction performance could be further ascribed to the improved hardness, seashell addition, and the bonding strength of the binder added [22]. Generally, the coefficient of friction performance was similar to that of brake pads produced with palm kernel fibers ranging between 0.325–0.365 [12].

3.1.6. Thermal conductivity assessment
Based on the data presented in Figure 8, it can be inferred that the thermal conductivity of the produced brake pad increases with an increase in seashell content, as observed from sample B to E. The drop in
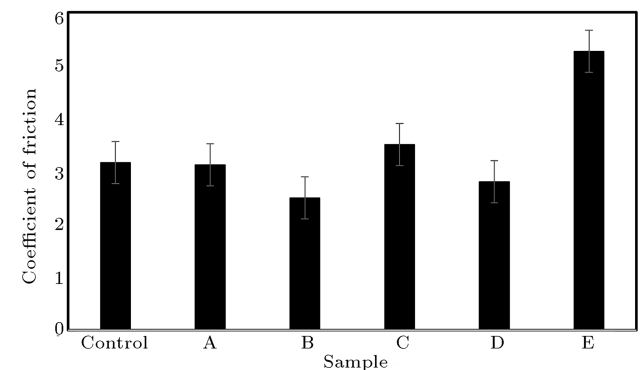
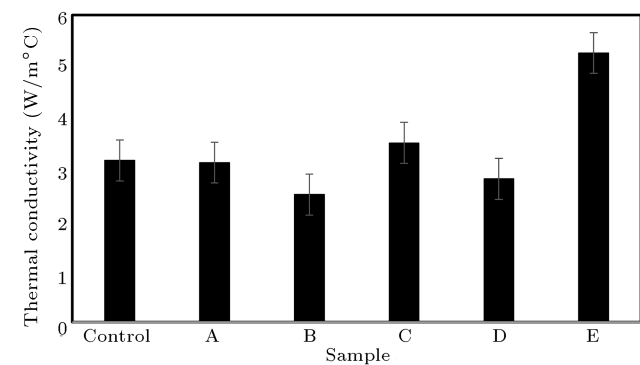**Figure 7.** Comparison of coefficient of friction of the produced samples with the control brake pad.

Figure 6. Comparison of specific wear rate of the produced samples with the control brake pad.

Figure 8. Comparison of thermal conductivity of the produced samples with the control brake pad.
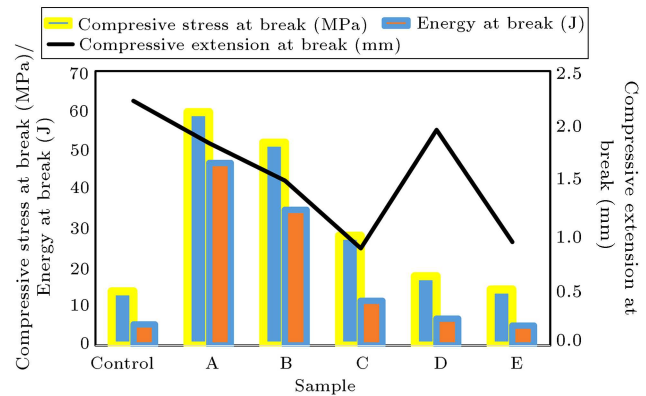
Table 4. Elemental composition of samples.

Element	Sample A (% wt)	Sample D (% wt)	Sample E (% wt)	Sample control (% wt)
Fe	66.634	59.230	67.552	88.759
C	5.715	7.016	5.959	4.990
Ag	3.083	3.556	3.473	<LOD
Ca	2.723	5.012	2.041	2.010
Pd	3.536	3.087	2.133	<LOD
Si	3.558	6.712	4.116	<LOD
Cd	5.093	5.351	4.949	<LOD
O	8.243	10.032	7.918	2.981
Co	1.415	<LOD	1.859	0.594
Cr	<LOD	<LOD	<LOD	0.576
Pb	<LOD	<LOD	<LOD	0.0905

thermal conductivity value at sample D is due to the optimum and proper arrangement of particles, making the sample less porous. The highest thermal conductivity of sample E is due to the oversaturation of the seashell in the composite, which is attributed to higher heat absorption [28]. The thermal conductivity of the control brake pad is 3.161 W/m°C, while the thermal conductivity of specimen D is 2.799 W/m°C. As a result, specimen D has higher heat resistance than the control sample. The thermal conductivity of maize-husk-based friction material was in the range of 0.251 to 0.372 W/mK for most agro-residue-based friction materials obtained from the literature. The cocoa-beans-shell-base brake pad was between 0.239 and 0.338, and the palm kernel shell-based friction material (1.460 W/mK) was reported by Dagwa and Ibhadode [30]. The results show that the seashell base brake pad will compete favorably with the existing non-asbestos based brake pads. The favorable performance of the brake pads in comparison to other options could be attributed to the absence or minimal occurrence of cracks or voids resulting from thermal stress caused by cyclic heating and cooling during the wear test [31].

3.1.7. Compressive assessment

It is observed from Figure 9 that the compressive strength of the produced brake pads decreased as the seashell content increased from samples A to E. This shows that the brittleness of the produced brake pads increased as seashell content increased, resulting in a decrease in the energy required to break the specimen. The proper and homogeneous arrangement of particles in sample D is considered responsible for its higher compressive extension at failure compared to the other samples. Sample D exhibited a compressive stress, extension, and energy at break of 17.74132 MPa,

Figure 9. Comparison of compressive strength of the produced samples with the control sample.

1.96356 mm, and 6.90480 J, respectively, whereas the control friction material had values of 13.83705 MPa, 2.22931 mm, and 5.44598 J.

3.1.8. Scanning electron microscope and XRF analysis

Figure 10 shows the arrangement of particle distribution in the produced friction material and the control sample. Most of the dark sides from Figure 10(a) and (b) show the presence of carbon, silicon, and some iron. Silicon carbide is known to be one of the hardest materials. Therefore, this is attributed to the hardness of the material [32]. The major constituents of the white areas are calcium carbonate and iron, as also observed in [1]. Calcium carbonate offers the advantage of a lower weight and a high melting point of 850°C [32]. Microfilm formation by $CaCO_3$ improves the wear resistance of the brake pad composite [28]. The significant elements found in the materials are presented in Table 4. The particle arrangement in the composite friction materials increased hardness as the seashell particle in the samples increased.
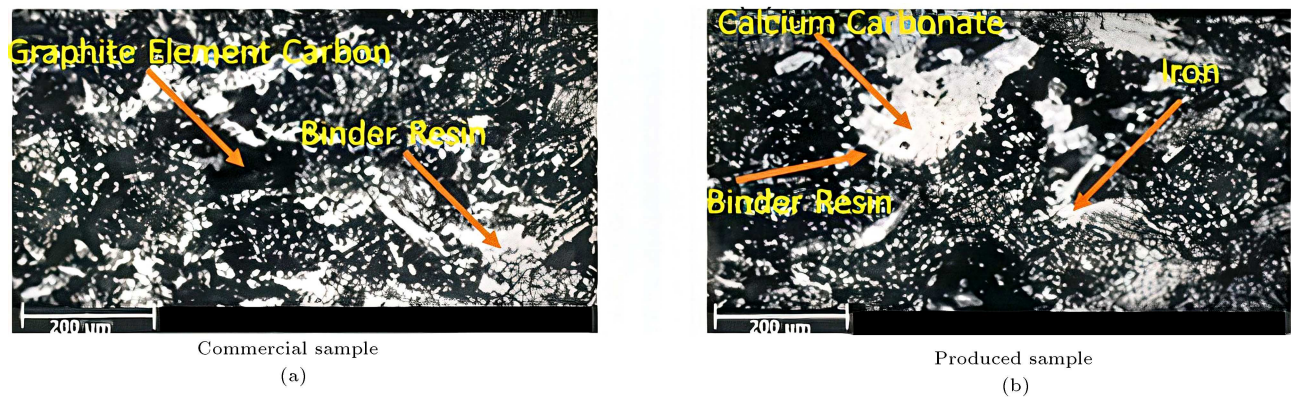
Figure 10. Microstructure analysis of (a) control/commercial sample and (b) sample D.

4. Conclusion

The results of the study indicate that seashells possess properties suitable for producing friction material for brake pads, as evidenced by their performance similarity to that of a commercially produced brake pad. The hardness, wear resistance, and compressive strength of the produced sample are all important factors in brake pad production, and sample D performed admirably. Increased seashell content in the formulation resulted in a decrease in sample density, water absorption, oil absorption, and thermal conductivity.

The findings of this study indicated that seashell, in conjunction with additives, could be used effectively as a replacement for asbestos-lined friction material for brake pads with no known health consequences.

Nomenclature

μ	Coefficient of friction
$a = g$	Acceleration due to gravity $(\mathrm{m/s^2})$

References

1. Elzayady, N. and Elsoeudy, R. "Microstructure and wear mechanisms investigation on the brake pad", *J. Mater. Res. Technol.*, **11**, pp. 2314–2335 (2021).

2. Kumar, S. and Ghosh, S.K. "Particle emission of organic brake pad material: A review", *J. Automob. Eng.*, pp. 1–11 (2019).

3. Maleque, M.A., Atiqah, A., Talib, R.J., et al. "New natural fibre reinforced aluminium composite for automotive brake pad", *Int. J. Mech. Mater. Eng.*, **7**, pp. 166–170 (2012).

4. Kumar, S. and Ghosh, S.K. "Porosity and tribological performance analysis on new developed metal matrix composite for brake pad materials", *J. Manuf. Process.*, **59**, pp. 186–204 (2020).

5. Singh, T. and Patnaik, A. "Performance assessment of lapinus-aramid based brake pad hybrid phenolic composites in friction braking", *Arch. Civ. Mech. Eng.*, **5**, pp. 151–161 (2014).

6. Achebe, C.H., Chukwuneke, J., and Anene, F.A. "A retrofit for asbestos-based brake pad employing palm kernel fiber as the base filler material", *J. Mater. Des. Appl.*, pp. 1–8 (2018).

7. Mausam, K., Sharma, A., and Singh, P.K. "Materials today: Proceedings calculating stress , temperature in brake pad using ANSYS composite materials", *Mater. Today Proc.*, **45**, pp. 3547–3550 (2021).

8. Ozdemir, A.O. and Karata, C. "Experimental determination of fracture toughness of woven/chopped glass ber hybrid reinforced thermoplastic composite laminates", *Sci. Iran.*, **28**, pp. 2202–2212 (2021).

9. Pujari, S. and Srikiran, S. "Experimental investigations on wear properties of palm kernel reinforced composites for brake pad applications", *Def. Technol.*, **15**, pp. 295–299 (2019).

10. Lawal, S.S., Bala, K.C., and Alegbede, A.T. "Development and production of brake pad from sawdust composite", *Leonardo J. Sci.*, **30**(1), pp. 47–56 (2017).

11. Sukrawan, Y. and Mardani, S.A. "Effect of bamboo weight faction on mechanical properties in non-asbestos composite of motorcycle brake pad", *Mater. Phys. Mech.*, **42**, pp. 367–372 (2019).

12. Krishnan, G.S., Babu, L.G., Pradhan, R., et al. "Study on tribological properties of palm kernel fiber for brake pad applications", *Mater. Res. Express.*, **7**, pp. 1–7 (2020).

13. Bin Wan Mohammad, W.A.S., Othman, N.H., Wan Ibrahim, M.H., et al. "A review on seashells ash as partial cement replacement", *IOP Conf. Ser. Mater. Sci. Eng.*, **271** (2017).

14. Bernard, S.S. and Jayakumari, L.S. "Pressure and temperature sensitivity analysis of palm fiber as a biobased reinforcement material in brake pad", *J. Brazilian Soc. Mech. Sci. Eng.*, **40**, pp. 1–12 (2018).

15. Krishnan, G.S., Jayakumari, L.S., Babu, L.G., et al. "Investigation on the physical, mechanical and tribological properties of areca sheath fibers for brake pad applications", *Mater. Res. Express.*, **6**, pp. 1–8 (2019).

16. Kumar, S. and Ghosh, S.K. "Statistical and artificial neural network technique for prediction of performance in AlSi$_{10}$Mg-MWCNT based composite materials", *Mater. Chem. Phys.*, **273**(125136), pp. 1–13 (2021).

17. Kumar, S. and Ghosh, S.K. "Statistical and computational analysis of an environment-friendly MWCNT/NiSO4 composite materials", *J. Manuf. Process.*, **66**, pp. 11–26 (2021).

18. Aweda, J.O., Omoniyi, P.O., and Ohijeagbon, I.O. "Suitability of pulverized cow bones as a paving tile constituent", *2nd Int. Conf. Eng. a Sustain. World, IOP Conference Series*, Ota, 012046 (2018).

19. Ohijeagbon, I.O., Adekunle, A.S., Omoniyi, P.O., et al. "Impact of production methods on some engineering properties of interlocking tiles", *Adeleke Univ. J. Eng. Technol.*, **2**, pp. 99–108 (2019).

20. Elakhame, Z.U., Jimoh, S.O., and Bankole, L.K. "Production and characterization of asbestos free brake pads from kenaf fiber composite", *Adeleke Univ. J. Eng. Technol.*, **3**, pp. 69–78 (2020).

21. Omoniyi, P.O., Ohijeagbon, I.O., Aweda, J.O., et al. "Investigation of brinell hardness and compressive strength of pulverized cow bones and lateritic paving tiles", *Adeleke Univ. J. Eng. Technol.*, **1**, pp. 59–69 (2018).

22. Edokpia, R.O., Aigbodion, V.S., Atuanya, C.U., et al. "Experimental study of the properties of brake pad using egg shell particles-Gum Arabic composites", *J. Chinese Adv. Mater. Soc.*, **4**, pp. 172–184 (2016).

23. ASTM G99 "Standard test method for wear testing with a pin-on-disk apparatus 1", *Astm Int.*, **05**, pp. 1–6 (2017).

24. Popoola, O.T., Rabiu, A.B., Ibrahim, H.K., et al. "Production of automobile brake pads from palm kernel shell, coconut shell, seashell and cow bone", *Adeleke Univ. J. Eng. Technol.*, **4**, pp. 92–101 (2021).

25. Omoniyi, P., Ohijeagbon, I., Aweda, J., et al. "Experimental data on the compressive and flexural strength of lateritic paving tiles compounded with pulverized cow bone", *Data Br.*, **33**, pp. 4–11 (2020).

26. Omoniyi, P.O., Aweda, J.O., Ohijeagbon, I.O., et al. "Modeling and simulation of mechanical properties of pulverized cow bone and lateritic paving tiles", *Stavebni Obz.-Civ. Eng. J.*, **29**, pp. 551–558 (2020).

27. ASTM D3410/D3410M "Standard test method for compressive properties of polymer matrix composite materials", *ASTM Int.*, **03**, pp. 1–13 (2016).

28. Park, J., Gweon, J., Seo, H., et al. "Effect of space fillers in brake friction composites on airborne particle emission: A case study with BaSO$_4$, Ca(OH)$_2$, and CaCO$_3$", *Tribol. Int.*, **165**(107334) (2022).

29. Ezekiel, I.O. and Inambao, F. "The effect of carbon nanospheres on the properties of bio-based hybrid nanocomposite brake pad materials", *Int. J. Mech. Prod.*, **11**, pp. 37–52 (2021).

30. Ibhadode, A.O.A. and Dagwa, I.M. "Development of asbestos-free friction lining material from palm kernel shell", *J. Brazilian Soc. Mech. Sci. Eng.*, **30**, pp. 166–173 (2008).

31. Borawski, A. "Testing passenger car brake pad exploitation time's impact on the values of the coefficient of friction and abrasive wear rate using a pin-on-disc method", *Materials (Basel).*, **15**, pp. 1–16 (2022).

32. Kumar, V.V. and Kumaran, S.S. "Friction material composite: Types of brake friction material formulations and effects of various ingredients on brake performance - a review", *Mater. Res. Express.*, **6**, pp. 1–15 (2019).

Biographies

Adebayo Adekunle is a Lecturer at the Department of Mechanical Engineering, University of Ilorin, Nigeria. His research interests include mechanical design, fabrication, and production engineering. He is a registered professional engineer with the Council for the Regulation of Engineering in Nigeria (COREN).

Mojeed Okunlola completed his Master's degree at the Department of Mechanical Engineering, University of Ilorin. His research interests include composite engineering, simulation, and modeling of composite materials.

Peter Omoniyi is a Lecturer at the Department of Mechanical Engineering, University of Ilorin. He is a registered professional engineer with the Council for the Regulation of Engineering in Nigeria (COREN). He has published several articles in the area of composite engineering, fusion welding, and additive manufacturing.

Adekunle Adeleke is a Lecturer at the Nile University of Nigeria, Abuja, Nigeria. He is a registered professional engineer with the Council for the Regulation of Engineering in Nigeria (COREN). He is a prolific researcher and has published several articles in the field of composite engineering.

Peter Ikubanni is currently a Lecturer at the Department of Mechanical Engineering, Landmark University, Nigeria. He is a registered professional engineer with the Council for the Regulation of Engineering in Nigeria (COREN). He has authored several publications in the area of composite engineering.

Tajudeen Popoola is currently a Lecturer at the Department of Mechanical Engineering, University of Ilorin. He is a registered professional engineer with the Council for the Regulation of Engineering in Nigeria

(COREN). He has authored several articles in the area of composite engineering, simulation, and modeling of engineering problems.

Hassan Ibrahim is a Lecturer at the Department of Mechanical Engineering, University of Ilorin. He is a registered professional engineer with the Council for the Regulation of Engineering in Nigeria (COREN). His major research focus is in the area of material characterization and composite engineering.